DOI: 10.1002/chem.200801732

Complex Long-Range Magnetic Ordering Behaviors in Anisotropic Cobalt(II)–Azide Multilayer Systems

En-Qing Gao,*[a] Pei-Pei Liu,[a] Yan-Qin Wang,[a] Qi Yue,[a] and Qing-Lun Wang[b]

Abstract: The crystal structures and magnetic properties of two new Co^{II} molecular magnets, $[Co(N_3)_2(btzb)]$ (**1**) and $[Co(N_3)_2(btze)_2]$ (**2**), are described and discussed (btzb = 1,4-bis(tetrazol-1-yl)butane and btze = 1,4-bis(tetrazol-1-yl)ethane). In the materials, (4,4) layers with μ-1,3-azide bridges are cross-linked by the monolayered btzb bridging ligands or spaced by bilayered btze terminal ligands to give a 3D (**1**) or 2D (**2**) coordination network with significantly different interlayer separations (10.6 vs. 15.2 Å). The observation that the layers in **1** and **2** are almost identical have not only allowed us to determine how the interlayer separation imposes its influences on their magnetic behavior, but also helps us understand the complex magnetic behavior of each structure. In the high-temperature range (> 25 K), almost identical magnetic behaviors, typical of 2D antiferromagnetic systems, are observed for **1** and **2**. At low temperature they exhibit unusual and different behaviors that combine spin canting (weak ferromagnetism), metamagnetism, and stepped hysteresis. It has been found that the interlayer separation has little influence on the ordering temperature (23 vs. 22 K), but imposes very-strong influence on the metamagnetic critical field (6500 vs. 450 Oe), the coercivity (7500 vs. 650 Oe), and the hysteresis-step size. It may also play an adjusting role in determining the canting angle. Taking into account the strong anisotropy of the systems and the interlayer dipolar interactions, we have reasonably interpreted the unusual metamagnetic and hysteresis behaviors and the differences between **1** and **2**. In particularly, the stepped hysteresis loops have been explained by two weak ferromagnetic states.

Keywords: azides · cobalt · magnetic properties · metamagnetism · spin canting

Introduction

The field of molecular magnets has attracted much attention and seen great progress in recent years.[1] The most majority of molecular magnets studied so far consist of extended coordination networks or discrete polynuclear clusters in which paramagnetic metal ions are held in close proximity by short bridging ligands, which allow for sufficiently strong magnetic exchange. The structures may be varied or tailored by incorporating different auxiliary ligands. Given the considerable diversity of coordination and supramolecular chemistry and the powerful tool of crystal engineering, chemists in this field have been able to obtain many new magnetic materials, for example, the newly-emerged single-molecule and single-chain magnets.[2] Additionally, these materials have offered great opportunities to better understand fundamental magnetic phenomena, such as long-range ordering (LRO), spin canting, metamagnetism, anisotropy, relaxation dynamics, and quantum tunneling of magnetization.[2a] As far as LRO is concerned, some complex and exotic behaviors have been revealed in molecular systems, for example, the presence of multiple areas of bistability or multi-stepped hysteresis,[3] and the combination of magnetic properties and other functions.[4]

The diversities of molecular-magnetic materials in structure and magnetism have been well illustrated by metal-azide systems.[5–11] The azide ion can adopt various bridging modes (μ-1,1, μ-1,3, μ-1,1,1 etc.), and can efficiently mediate ferro- (F) or antiferromagnetic (AF) coupling. By incorporating different organic ligands, a large variety of polymeric metal-azide compounds with different magnetic behaviors have been reported. The metal-azide networks in these compounds are mostly one- (1D) and two-dimensional (2D), and rarely three-dimensional (3D).[7] In recent years, in the hope of enhancing the ORL behaviors, some 3D materials

[a] Prof. Dr. E.-Q. Gao, P.-P. Liu, Y.-Q. Wang, Dr. Q. Yue
Shanghai Key Laboratory of Green Chemistry and Chemical Processes, Department of Chemistry
East China Normal University, Shanghai 200062 (China)
Fax: (+86) 21-62233404
E-mail: eqgao@chem.ecnu.edu.cn

[b] Dr. Q.-L. Wang
Department of Chemistry
Nankai University, Tianjin 300071 (China)

 © 2009 Wiley-VCH Verlag GmbH & Co. KGaA, Weinheim WILEY InterScience DISCOVER SOMETHING GREAT

in which 2D azide-bridged layers are cross-linked by organic bridging ligands have been synthesized by us and others.[8,9] Generally speaking, the bulk magnetic properties of the multilayer compounds with large interlayer separations, whether the metal-azide layers are chemically isolated[10,11] or interlinked[8], are primarily dependent upon the interlayer structures, but can be dramatically influenced by the weak interlayer interactions. How does the interlayer interaction itself influence bulk magnetic properties? This is a fundamental question for the engineering of molecular magnetic materials. It is highly desirable to obtain a series of materials with identical metal-azide layers but different interlayer separations. Consequently, one can determine which influences are exclusively imposed by the interlayer factors on magnetic properties. This is a difficult task owing to the complexity of the metal-azide systems. Although the versatility of azide coordination offers us rich chemistry and magnetism, it also challenges crystal engineering. As shown by previous studies,[5,7e,8b,d] a minor variation in the coligand or synthetic conditions can unpredictably lead to significant changes in the metal-azide network, which may be reflected in intralayer parameters, the coordination mode, the topology or even the network dimensionality. For different layers with different interlayer separations, one cannot unambiguously determine whether (or to what extent) a change in bulk properties is owed to the variation in the interlayer factor. Therefore, although a number of metal-azide multilayer compounds have been synthesized,[8,10,11] the exact magnetic effects of interlayer changes are still waiting to be unveiled.[8a,b] Recently we have obtained two Cu^{II} compounds that consist of almost identical azide layers linked by organic ligands of different lengths.[8a] They both behave as metamagnets below $T_C = 4$ K, and it has been demonstrated that the influence of interlayer distances is only imposed on the metamagnetic critical fields.

Along this line, we focus our attention on Co^{II} systems, which usually possess strong magnetic anisotropy. It is known that anisotropy plays important roles in spin canting, metamagnetism,[12] hysteresis (coercivity),[13] and relaxation dynamics.[2] So Co^{II} systems often exhibit exotic magnetic behaviors.[3a,b,14] Although our previous work on the nearly isotropic Cu^{II}-azide systems has shown that the influence of the interlayer interaction is reflected in metamagnetic critical fields,[8a] it should be interesting to inspect how the interlayer interaction imposes its influences in the strongly anisotropic Co^{II}-azide system. On the other hand, compared to the weakly anisotropic M^{II}-azide systems (M = Mn, Ni and Cu),[5–10] the Co^{II} analogues[5d,8d,10f,11] are seldom studied. Systematic investigations on systems with almost identical intralayer factors but distinct interlayer factors would help us to better understand the magnetochemistry in the complex systems. In this paper, we report the syntheses, structure and magnetic properties of two new Co^{II} compounds, $[Co(N_3)_2(btzb)]$ (**1**, 3D structure, btzb = 1,4-bis(tetrazol-1-yl)butane) and $[Co(N_3)_2(btze)_2]$ (**2**, 2D structure, btze = 1,4-bis(tetrazol-1-yl)ethane). Both compounds exhibit complex magnetic behaviors combining spin canting (weak ferromagnetism), metamagnetism and exotic hysteresis. Fortunately, although different in overall network dimensionality, **1** and **2** contain almost identical layers and have distinct interlayer separations. This allows us to perform the magnetic analyses outlined above.

Results

Synthesis and IR spectra: The compounds are prepared by reacting cobalt chloride, sodium azide, and appropriate bis(tetrazole) ligands (btze and btzb) in aqueous solutions at room temperature. The reactions using btzb are somewhat insensitive to the starting Co:btzb molar ratio (1:2 or 1:1) and always give compound **1** with Co:btzb = 1:1. We were unable to synthesize a compound with Co:btze = 1:1. Instead, compound **2** was obtained by using the starting ratio Co:btze = 1:2. The phase purity of both compounds has been confirmed by powder X-ray diffraction. Both compounds exhibit a very strong IR band at about $\tilde{\nu} = 2075\ cm^{-1}$, owing to the $\nu_{as}(N_3)$ vibration. The medium band at about $\tilde{\nu} = 3130\ cm^{-1}$ is characteristic of the ν(C–H) vibration in the tetrazole ring.

Crystal structures: Compounds **1** and **2** have different stoichiometries and exhibit 3D and 2D coordination networks, respectively. However, they do crystallize in the same space group ($P2_1/c$) and contain almost identical 2D Co^{II}-azide layers, so the two structures are described together for the convenience of comparisons.

The coordination environments of the metal ion and ligands are shown in Figure 1. In both compounds, the unique metal ion resides at an inversion center and is coordinated by six nitrogen atoms from four azide ions and two bis(tetrazole) ligands. The N–Co–N angles are very close to 90° (from 88.1 to 91.9°), and the $Co–N_{tetrazole}$ bond distances [Co1–N4, 2.127(4) Å in **1** and 2.139(2) Å in **2**) fall between the asymmetric $Co–N_{azide}$ distances [about 2.10 (Co1–N1) and 2.16 Å (Co1–N3) in both compounds]. These structural parameters suggest a pseudo-octahedral geometry with slight elongation along one $N_{azide}–Co–N_{azide}$ axis and slight compression along the other $N_{azide}–Co–N_{azide}$ axis. The quasi-linear azide ions in each structure are all crystallographically equivalent and join neighboring metal ions in the μ-1,3 (or end-to-end, EE) bridging mode. Consequently, each metal ion is linked to four neighbors through four azide bridges to generate a 2D (4,4) layer parallel to the *bc* plane (Figure 2a). The layer has rhombic windows, with the acute Co···Co···Co angles being 65.2° in **1** and 64.6° in **2**. The Co–N–N–N-Co moiety has asymmetric Co–N bond lengths and Co–N–N angles and assumes a gauche conformation, as suggested by the Co–N···N–Co torsion angles (τ). All these parameters can impose influences on the magnetic behaviors.[5a] For clarity, the relevant parameters for **1** and **2** are summarized and compared in Table 1, together with those for the two previous compounds containing similar Co^{II}-azide layers.[8d,11] It turns out that **1** and **2** show only minor differences in the intralayer parameters, but the differences

 © 2009 Wiley-VCH Verlag GmbH & Co. KGaA, Weinheim

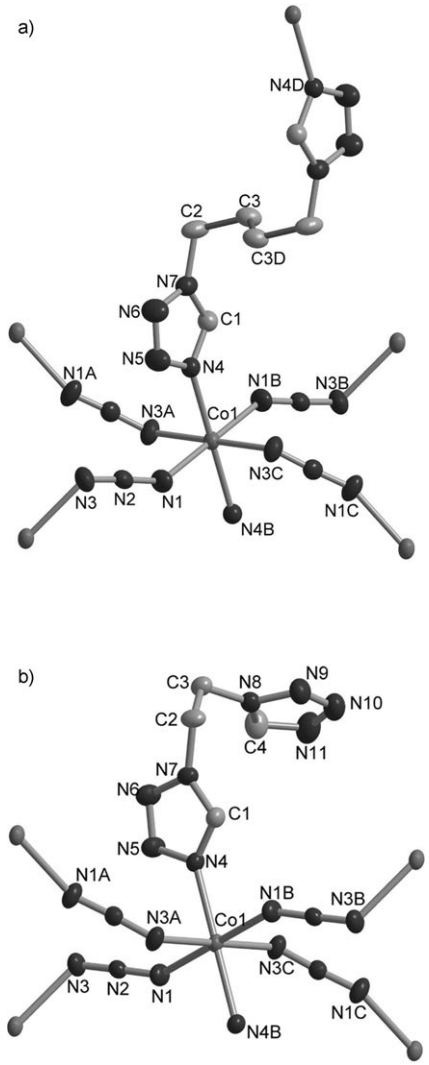

Figure 1. The coordination environments of the metal ion and ligands in compounds a) **1** and b) **2**. Symmetry code: A $1-x$, $0.5+y$, $1.5-z$; B $1-x$, $-y$, $1-z$; C x, $-0.5-y$, $-0.5+z$; D $2-x$, $1-y$, $1-z$.

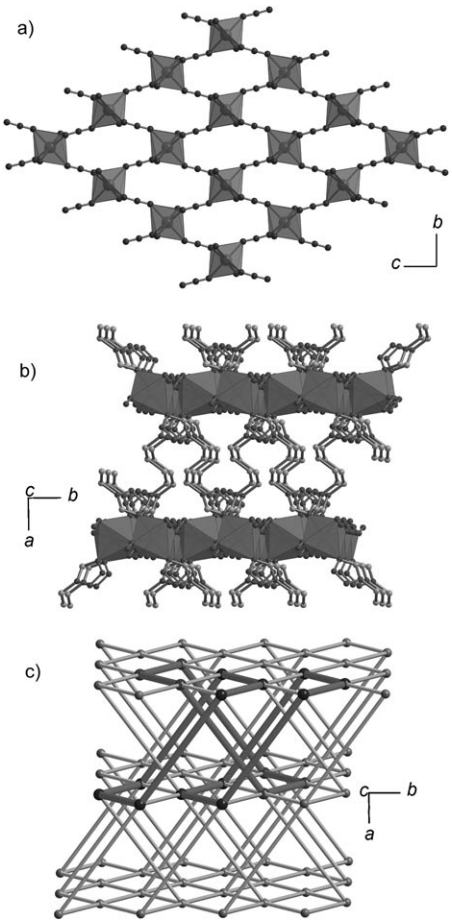

Figure 2. a) An azide-bridged (4,4) Co^{II} layer in **1**. The layer in **2** is similar. b) The 3D structure in **1**. c) The 3D net observed in **1**, where the self-penetration is highlighted by thicker dark gray rods.

from the previous compounds is somewhat more significant. An important difference lies in the coordination geometry: the axial elongation of the Co^{II} octahedron in **1** or **2** is along one of the N_{azide}–Co–N_{azide} linkages, whereas the elongation in the previous compounds is along N_L–Co–N_L (L represents the organic auxiliary ligands), with all the Co–N_{azide} bond lengths being shorter than Co–N_L. In all these compounds, the adjacent Co atoms bridged by azide are related by the crystallographic 2-fold screw axis, and this inevitably make the adjacent coordination polyhedrons slant with respect to each other. Thus, throughout the layer, two sets of relatively slanted polyhedrons alternate along the azide bridges. To characterize the relative slanting, we calculated the dihedral angles (δ) between neighboring [CoN_4] planes defined by azide nitrogen atoms. As expected, the dihedral angles are closely related to the Co–N···N–Co torsion angle (τ). As can be seen from Table 1, the τ and δ values for **1**

Table 1. Some structural and magnetic data for compounds with Co-azide (4,4) layers.

Compound[a]	**1**	**2**	**3**	**4**
M–N_{azide} [Å]	2.100(2), 2.158(4)	2.103(2), 2.158(3)	2.125, 2.133	2.113, 2.142
M–N_L [Å][b]	2.127(4)	2.139(2)	2.172	2.185
M–N–N [°]	145.65(16), 119.01(15)	146.15(13), 120.30(12)	149.2, 128.2	150.0, 121.1
$\tau_{M-N\cdots N-M}$ [°]	122.5	123.7	84.9	131.0
δ [°][c]	62.1	61.2	83.3	55.5
M···M [Å][d]	5.794	5.842	5.848	5.932
M···M [Å][e]	10.633	15.172	11.73	10.97
α [°][f]	6.4	9.9	15	5.2
T_C [K]	23	22	11	10
H_C [Oe][g]	6500	500	NA[h]	NA[h]
H_C [Oe][i]	7500	650	120	[j]
Ref.	this work	this work	[11]	[8d]

[a] Compound **3**: $[Co(N_3)_2(4acpy)_2]_n$, with 4acpy = 4-acetylpyridine; compound **4**: $[Co(N_3)_2(bpg)]_n$, with bpg = *meso*-α,β-bis(4-pyridyl)glycol. [b] N_L is the coordinated atom from appropriate organic ligands. [c] The dihedral angle between neighboring [CoN_4] planes defined by azide nitrogen atoms. [d] The distances spanned by the single azide bridge. [e] The shortest Co···Co distance between layers. [f] Spin-canting angle. The typical value of $g_{eff} = 4.3$ for Co^{II} [11b–12] was used for the estimation. [g] The critical field for metamagnetic transition at 2 K. [h] Not applicable. [i] Coercive field at 2 K. [j] Not reported.

 © 2009 Wiley-VCH Verlag GmbH & Co. KGaA, Weinheim

and **2** are very similar but evidently different from those for the previous compounds.

Despite of the similarity in layer structures, compound **1** and **2** differ in the interlayer sense. In **1**, each btzb ligand binds two Co^{II} ions from neighboring layers, and hence the inorganic Co^{II}-azide layers are pillared into a hybrid 3D architecture (Figure 2b). The organic ligands reside on inversion centers and assume a zigzag-like shape with the $(CH_2)_4$ spacer between tetrazole rings taking the GTG conformation (G = gauche, T = transoid). The centrosymmetric zigzag shape requires that the two metal polyhedrons it links be aligned in parallel. Therefore, to adapt to the two relatively slanted sets of coordination polyhedrons in the layers, the bridging ligands between the layers are also systematically slanted in two criss-cross directions. As a result, the shortest interlayer Co···Co distance (10.633(4) Å, equal to the *a*-axis of the unit cell) is much shorter than that spanned by the pillar (12.33 Å). Another result of the criss-cross arrangement of the bridging ligands is the occurrence of self-penetration in the net. Self-penetration (or self-catenation, self-entanglement) is a special type of supramolecular entanglements that is still a rare occurrence, but has evoked increasing interest in recent years.[15] The simplified 3D net is illustrated in Figure 2c. The short Schläfli symbol for this 6-connected net is $4^4 6^{10} 8$. Each 6-membered chair-like ring (the shortest interlayer circuit) involving two interlayer linkers (btzb) in one direction is threaded by two linkers in the other direction, resulting in self-catenation between the interlayer circuits (highlighted in dark gray in Figure 2c).

By contrast, the 2D layers in **2** are not linked into a 3D network, because the btze ligand ligates only one metal ion using one of its two tetrazole rings. The ligand assumes a gauche conformation with the N7–C2–C3–N8 torsion angle being 60.5° to give a bent shape that is incompatible with interlayer connection. The ligands stick out of each layer on both sides, and form an organic bilayer with no interdigitation and no evident interactions stronger than the van der Waals force. Consequently, as compared in Figure 3, the non-bridging btze ligand leads to a much larger interlayer spacing than the bridging btzb ligand, although btze is shorter. The shortest interlayer Co···Co distance is 15.17 Å, which is the longest of the known compounds with Co^{II}-azide layers (Table 1).

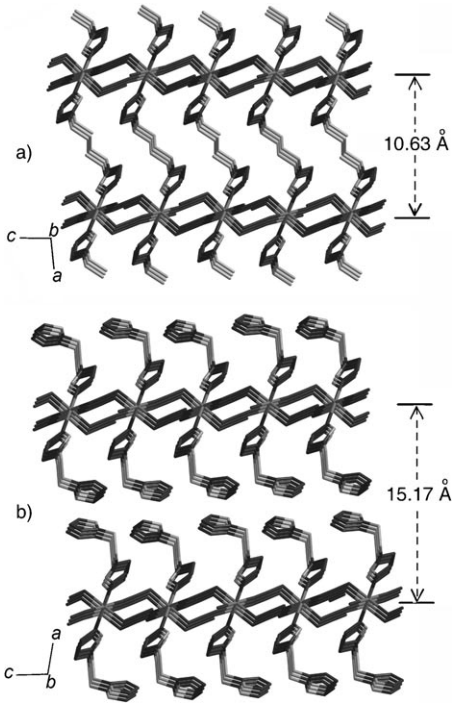

Figure 3. A comparison of the interlayer relationship in a) **1** and b) **2**. The distances refer to shortest interlayer Co···Co distances.

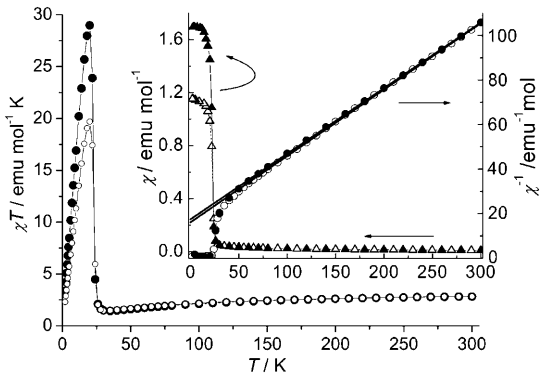

Figure 4. Thermal variation of magnetic susceptibilities of **1** (△, ○) and **2** (▲, ●) at 1 kOe, shown as χT, χ, χ^{-1} versus T plots. The solid straight lines in the inset are the fits to the Curie–Weiss law. Other lines are only a guide for the eye.

Magnetic properties: The magnetic susceptibilities (χ) of **1** and **2** were measured on polycrystalline samples under 1 kOe in the 2–300 K range (Figure 4). The two compounds display similar behavior, especially in the high-temperature range. The χT values per Co^{II} at 300 K are about 2.83 emu K mol^{-1} for both, in the normal range for octahedral Co^{II} with an unquenched orbital momentum. As the temperature is lowered, the χ value first increases smoothly, then rises abruptly in the region of 25–15 K, and finally approaches saturation upon further cooling. The values at 2 K are 1.15 and 1.69 emu mol^{-1} for **1** and **2**, respectively. On the other hand, the χT value first decreases smoothly to a minimum at about 30 K, then rises rapidly to a sharp maximum at 20 K (χT = 19.7 and 29.0 emu K mol^{-1} for **1** and **2**, respectively), and finally drops rapidly owing to saturation effects. The χ^{-1} versus T plots above 60 K follow the Curie–Weiss law with C = 3.36(3) emu K mol^{-1}, θ = −59.3(4) K for **1**, and C = 3.40(3) emu K mol^{-1}, θ = −54.2(3) K for **2**, respectively. The large negative Weiss constants (θ) and the initial decrease of χT could be a result of the concurrent operation of the spin-orbital coupling of Co^{II} ions, ligand field effects, and the AF coupling between adjacent Co^{II} ions through the EE azide bridges. However, the steep rises in χ and χT at low temperature clearly indicate that a kind of spontaneous magnetization emerges. This phenomenon in an AF system could be attributed to weak ferromagnetism, owing to spin canting (also called "canted antiferromagnetism"):[12] the AF cou-

 © 2009 Wiley-VCH Verlag GmbH & Co. KGaA, Weinheim

pled spins from different sublattices are not perfectly antiparallel, but canted to each other, and the resulting net moments are correlated in a ferromagnetic-like fashion and develop into LRO below the critical temperature.

To characterize the low-temperature behaviors of **1** and **2**, FC (field-cooled) and ZFC (zero-field-cooled) magnetization measurements were performed under different fields (Figure 5, both $M(T)$ and $\chi(T)$ ($\chi = M/H$) curves are plotted

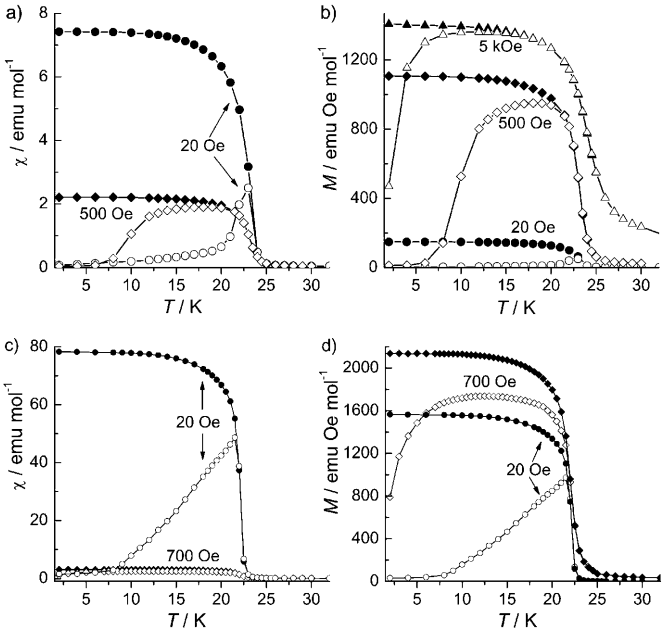

Figure 5. The χ and M versus T plots of zero-field-cooled (△, ○) and field-cooled (▲, ●) magnetizations for **1** (a and b) and **2** (c and d) at different fields. The lines are a guide for the eye.

to reveal the details). As expected for spin canted systems, the low-temperature FC susceptibilities for both compounds are strongly dependent upon the field applied, and the values at 20 Oe are much higher than those at higher fields (Figure 5a,c). At all the fields measured, the FC magnetization rises rapidly below ≈25 K and approaches the saturation value below 20 K, suggesting that the field-cooling procedure creates a weak ferromagnetic (WF) state in which the spin-canted AF layers are ferromagnetically ordered (F-ordered). The critical temperatures were estimated to be $T_c = 23.0(1)$ K (**1**) and 22.1(1) K (**2**), at which the FC dM/dT derivative curves exhibit sharp minima. The T_c values are confirmed by the observation that the ZFC and FC curves measured at 20 Oe merge at 23 K for **1** and 22 K for **2**. Notably, the FC saturation magnetization of **2** is higher than that of **1** under the same field. The difference is more evident at lower filed, and at 20 Oe and below 20 K, the FC value of **2** is 10 times higher than that of **1** (compare Figure 5a and c). For both compounds, the initial ZFC magnetization at 20 Oe is very weak, increases very slowly upon warming up to 19 K for **1** and 8 K for **2**, and then undergoes a rapid increase merge into FC curves at T_c. Similar behaviors were also observed for 1 at 500 Oe, but the rapid rise of the ZFC magnetization begins earlier (at lower temperature, 6 K). At higher fields (5 kOe for **1** and 700 Oe for **2**), the ZFC magnetization increases rapidly to the maximum value upon warming from 2 K. These observations may suggest that an AF-ordered state is reached in the ZFC sample and can undergo a field-induced metamagnetic transition. This will be commented in the discussion section.

The thermal dependence of the ac susceptibilities of **1** and **2** were measured at frequencies 1, 10, 100, and 1000 Hz. As can be seen from Figure 6, both in-phase (χ') and out-of

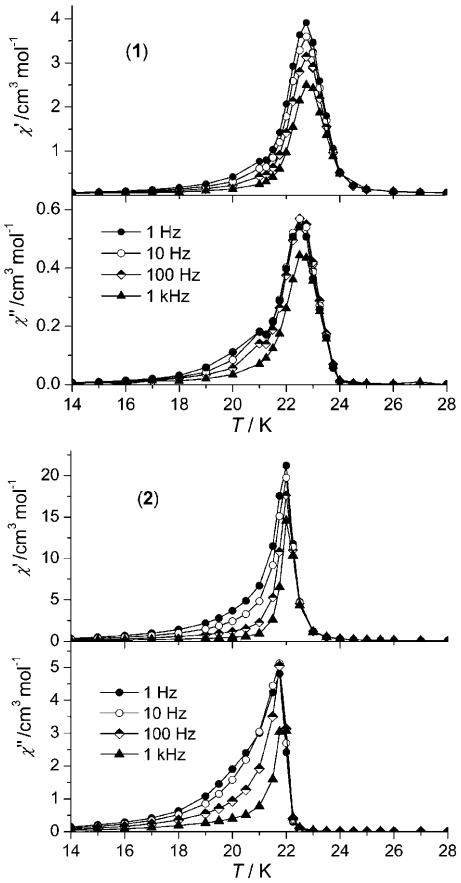

Figure 6. Thermal dependence of the real (χ') and imaginary components (χ'') of the ac susceptibilities of **1** and **2** at different frequency. The lines are a guide for the eye.

-phase components (χ'') of the susceptibilities exhibit maxima at about 22.7 K for **1** and 21.9 K for **2**, close to the T_c values), and the maximum position is independent of frequency. This confirms the occurrence of ferromagnetic-like LRO. As found in dc measurements, **2** gives much stronger ac signals than **1**. It is noted that the χ' and χ'' peaks at 1, 10, and 100 Hz are unsymmetrical in shape, with the low-temperature sides showing some dependence upon the frequency (it is less appreciable in **1**). This indicates the presence of some dynamic relaxation process. The fact that the χ' and χ'' peaks at the high frequency of 1 kHz are almost

 © 2009 Wiley-VCH Verlag GmbH & Co. KGaA, Weinheim

symmetric may suggest that the alternation of the ac field at 1 kHz is too fast to evoke the dynamic process. As a tentative explanation, we presume that the dynamic behavior arises from the restricted movement of domain walls upon approaching T_c. Further studies are needed to clarify the exact mechanism.

Further information comes from the field-dependent isothermal magnetization measurements (Figure 7). For both compounds, the magnetization at 2 K increases slowly and linearly with the field at high field region, and the values of 0.52 Nβ (**1**) and 0.58 Nβ (**2**) at 50 kOe is far from saturation. These features are consistent with the AF nature of the intralayer interactions between neighboring metal ions. The saturation magnetization (M_s) for a pseudoctahedral Co^{II} ion at very low temperature (<20 K) is usually 2.1–2.5 Nβ with $S_{eff}=1/2$ and $g_{eff}=4.1$–5.0.[3b,16] Extrapolating the high-field linear parts of the magnetization curves to zero field give magnetization values of 0.24 and 0.37 Nβ for **1** and **2**, respectively. Taking the values as the magnetization (M_w) arising from spin canting, the canting angle (α) could be estimated to be in the ranges of 5.5–6.6° for **1** and 8.5-10.1° for **2**, according to the equation $\sin\alpha = M_w/M_s$. The values are among the largest canting angles reported for weak ferromagnets.[11b,17] The larger canting angle for **2** is consistent with its higher values of FC saturation magnetization and ac susceptibility. As shown in Figure 7, the initial $M(H)$ curve measured on a ZFC sample of **1** exhibits the sigmoid shape typical of metamagnetism, which is often observed in layer or chain systems with anisotropy and competing interactions:[12] The slow increase of magnetization in the low field region (0–2.5 kOe) suggests the AF ordering of the spin-canted layers, and the rapid rise in the 3–9 kOe region indicates that the interlayer AF ordering can be broken up by the applied field to generate a WF state in which the spin-canted layers are F-ordered. The critical field for the AF-to-F transition at 2 K was estimated to be 6.5 kOe, at which the dM/dH curve exhibits a maximum. A blow-up (Figure 7b, inset) of the low field region of the initial $M(H)$ curve of **2** also suggests metamagnetism, but the critical field is much lower (500 Oe).

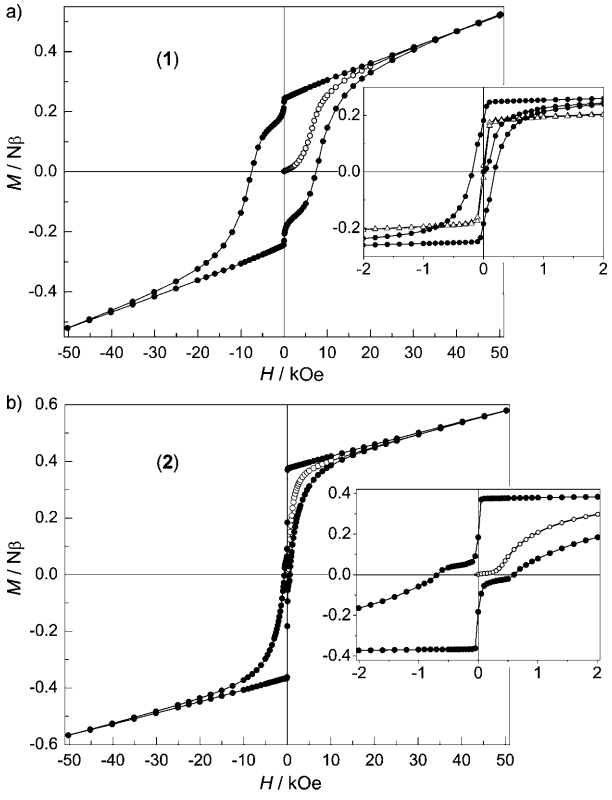

Figure 7. a) Isothermal magnetization of **1** at 2 K (○: initial magnetization, ●: loop). Inset: magnetization plots for **1** at different temperatures (●: 15 K and △: 22 K). b) Isothermal magnetization of **2** at 2 K (○: initial magnetization, ●: loop). Inset: The low-field blow-up of the plot for **2** at 2 K. The lines are a guide for the eye.

At 2 K, both compounds exhibit hysteresis loops, related to the anisotropy of Co^{II}. Compound **1** behaves as a hard magnet with a large coercive field of 7.5 kOe and a remnant magnetization of 0.23 Nβ (1.3×10^3 cm^3 Oe mol^{-1}), whereas **2** is much softer, with a much smaller coercive field (650 Oe) and a comparable remnant magnetization (0.18 Nβ = 1.0×10^3 cm^3 Oe mol^{-1}). The large coercive field for **1**, to our knowledge, is the highest for azide-derived materials.[5,7–11] A notably feature common to the two materials is that the hysteresis loop exhibits two reproducible steps when sweeping the field from one end to the other end of the loop. The first step occurs in a narrow range (±100 Oe for **1** and slightly narrower for **2**) across the zero field, whereas the second step crosses the $M=0$ axis and corresponds to the reversal of magnetization, with the critical fields (≈± 8.0 kOe for **1** and ±700 Oe for **2**, estimated from the maxima of the dM/dH curves) being close to the coercive fields. The step size (the magnitude of magnetization decrease) of the first step for **2** (0.37 to 0.06 Nβ) is much larger than that (0.24 to 0.20 Nβ) for **1**.

Isothermal magnetization plots were also obtained at 15 and 22 K for **1** (Figure 7a, inset). At 15 K, the metamagnetic transition is still evident from the low-field sigmoid shape of the initial $M(H)$ curve, but the critical field is reduced to a much smaller value (≈150 Oe, only one fortieth of the value at 2 K), The steps in the hysteresis loop are still present but nearly indiscernible. The coercive field is also much weaker (180 Oe) than that at 2 K, although the remnant magnetization (0.18 Nβ) is comparable. At 22 K, the metamagnetic characteristic disappears, and instead, the initial magnetization increases very rapidly in the field range from 0 to 100 Oe, as observed for a simple weak ferromagnet. The steps in the hysteresis loop also disappear, and the coercive field and the remnant magnetization are negligibly small.

Discussion

We have described two inorganic-organic hybrid compounds with almost identical Co-azide layers but distinct interlayer separations defined by monolayered bridging ligands (**1**)

 © 2009 Wiley-VCH Verlag GmbH & Co. KGaA, Weinheim

and bilayered non-bridging ligands (**2**). In the high-temperature range (>25 K) the two compounds exhibit almost identical magnetic behaviors, characteristic of 2D AF systems, simply reflecting their similarity in layer structures and the weakness of interlayer interaction. However, at low temperatures, they exhibit complex and different LRO behaviors combining spin canting, metamagnetism, and stepped hysteresis.

Of primary importance is the spin canting. Generally, spin canting can arise from two mechanisms:[18] i) The antisymmetric Dzyaloshinsky-Moriya (DM) interaction, which energetically favors the perpendicular alignment for the interacting spins; ii) different anisotropy axes at neighboring metal sites, which energetically favors the canting of neighboring spins with respect to each other. Both mechanisms require that the relevant metal sites cannot be related by a center of symmetry and the DM mechanism also requires g-factor anisotropy. It is well known that pseudo-octahedral Co^{II} has strong magnetic anisotropy (including resulting from unquenched orbital momentum and spin-orbit coupling. In the layers of **1** and **2**, neighboring Co^{II} ions are not related by a center of symmetry and their coordination polyhedrons (hence the anisotropy axes) are slanted with respect to each other. Therefore, both mechanisms favor a spin-canting structure for the Co^{II}-azide layer. Interlayer interactions may evoke 3D magnetic ordering. The F ordering of the spin-canted layers generates a WF state, whereas the AF ordering generates an AF state, in which the canting is hidden. Metamagnetism occurs if the AF state changes into a WF state under a sufficiently strong field. As will be shown, **1** and **2** exhibit more complex behaviors than a typical metamagnet.

Before discussing the metamagnetic behavior, we would like to give some remarks on the ordering temperature. Despite the distinct interlayer distances in **1** and **2** (10.6 vs. 15.2 Å), the two compounds have similar T_C values (23 vs. 22 K). LRO in molecular materials can be evoked by i) quantum exchange interaction mediated through bridges, hydrogen bonds or conjugated π electrons, and ii) through-space dipolar interactions. The former interaction, which is known to vanish extremely rapidly with the distance, can hardly justify the relative high T_C and its insensitivity to intralayer spacing. Considering the large interlayer spacing in **1** and **2**, the saturated $(CH_2)_4$ linker in **1** and the weak van der Waals interlayer force, the LRO behaviors observed here should be promoted by dipolar interactions, which have long-range effects.[19a] It has been proposed that the dipole interaction between layers leads to 3D ordering when the intralayer correlation length reaches a threshold value.[19b] Because the correlation length diverges exponentially with the temperature, the temperature at which the threshold is reached depends only weakly upon interlayer spacing, but mainly upon the divergence rate of the intralayer correlation length, which in turn depends upon intralayer magnetic exchange. This model has been proposed to explain the ordering of the ferromagnetic layers in compounds $Cu_2(OH)_3(RCOO)$,[19] and it seems applicable to the present WF Co^{II}-azide systems in which the intralayer correlation length should depend upon the intralayer factors including AF exchange, antisymmetric exchange and other factors that can influence the spin canting structure.

It could be informative to include other compounds with Co^{II}-azide (4,4) layers in the discussion. Only two have been reported previously: one (**3**) is 2D with 4-acetylpyridine as non-bridging interlayer spacers,[11] and the other (**4**) is 3D with *meso*-α,β-bis(4-pyridyl)glycol as interlayer linkers.[8d] The relevant magneto-structural data are listed in Table 1. As can be seen, **3** and **4** show some evident intralayer differences from **1** and **2**, with the interlayer distances being slightly larger than that in **1**, and they also exhibit weak ferromagnetism as result of spin canting, but with much lower T_C values. This confirms that T_C values for these compounds are almost independent of interlayer spacing, but dependent upon intralayer structure. Because of the rarity of the examples and the complexity arising from spin canting and Co^{II} anisotropy, we cannot conclude any warranted magneto-structural correlations between the T_C values and the intralayer parameters.

Now let us return to the topic of the metamagnetic behaviors. The ZFC $M(T)$ and $M(H)$ curves of **1** and **2** can be easily understood by considering that a sufficiently strong field can induce a metamagnetic transition from AF to WF states, but the FC $M(T)$ curves are atypical of metamagnets. The low-filed FC $M(T)$ curve for a metamagnet usually shows a maximum, owing to the magnetic transition from paramagnetic to AF ordering. The maximum disappears if the applied field is strong enough to prevent AF ordering but induce F ordering. However, the FC curves of **1** and **2** show no decrease down to 2 K even at a field much lower than the critical field. This does not really contradict metamagnetism, and can be well explained by assuming that the AF state generated in the ZFC samples and the WF state in FC samples are both stabilized by internal anisotropy fields. As mentioned, here the interlayer magnetic ordering is driven by dipolar interactions, which is strongly anisotropic in nature.[19a] Such interactions, in combination with the intralayer interactions and single-ion anisotropy, set up an anisotropy field in the ordered state. The anisotropy field stabilizes the state and has to be overcome to break up the interlayer ordering. The anisotropy field can reach a significant strength at very low temperature (as evidenced by the high metamagnetic critical field of **1** at 2 K), but it decreases very rapidly as temperature increases (as evidenced by the much lower critical field of **1** at 15 K) as a result of the thermal effects on correlation length and anisotropy. Actually, the $M(H)$ curve of **1** at 22 K does not show discernible metamagnetic characteristics, and the magnetization increases very rapidly upon applying a weak field. This suggests that the AF ordering is not set on at around T_C. Therefore, when a field-cooling procedure is applied, a very low field can induce the F ordering of the layers at T_C. Once generated, the WF state is stabilized by an internal anisotropy field, which also increases rapidly upon cooling and prevents the state from changing into the AF state. The stability of the

 © 2009 Wiley-VCH Verlag GmbH & Co. KGaA, Weinheim

WF state is confirmed by hysteresis measurements. Once magnetized, the WF state does not revert to the original AF state upon lowering the field to zero (see below). To finish the discussion on metamagnetism, we comment that the difference between **1** and **2** in critical field is evidently attributed to their difference in interlayer spacing: an increase in the interlayer separation leads to a remarkable reduction in the anisotropy field, and hence a lower critical field is needed to break up the AF ordering. This is consistent with the previous finding on Cu^{II} systems,[8a] but here the spacing dependence is much more significant. In the previous Cu^{II} systems, the spacing increase from 10.9 to 11.6 Å leads to a variation of the critical field from 700 and 300 Oe, By contrast, the spacing increase from 10.5 to 15.2 Å in the present system leads to a reduction of the critical field from the large value of 6.5 kOe to as small as 450 Oe. It is apparent that the different anisotropy of Cu^{II} and Co^{II} is important in determining the metamagnetic properties and their dependence on interlayer spacing.

It is worth noting that the hysteresis loops of **1** and **2** at 2 K exhibits two reproducible steps when sweeping the field from one end to the other end, the first around zero field and the other close to the coercive filed. This feature has been observed for two hydroxide-bridged Co^{II} layer compounds, but no interpretation was provided.[20] This could not be due to small admixture of an impurity phases, considering that the bulk phase purity has been confirmed by X-ray diffraction and that the steps in **1** and **2** are quite evident and very different. The differences between the two compounds lie in step sizes (decreases in magnetization) and the second-step positions (coercive fields) step. It is well known that some single-molecule magnets show hysteresis steps at zero and non-zero fields with regular intervals, owing to QTM through the anisotropy barrier.[2a] This is not the case here. Here we propose a tentative interpretation as follows, which explains not only the occurrence of the steps but also the differences between **1** and **2**. The basic idea is that there are two different WF states. i) The field-induced metamagnetic transition from the AF state generates a WF1 state, for which the magnetization is stabilized by the external field. ii) When the applied field is switched off, the WF1 state relaxes to a different WF state (WF2) with smaller magnetization (roughly 0.20 Nβ for **1** and 0.06 Nβ for **2**), perhaps by some reorientation of microdomains. This is the zero-field step (WF1→WF2). iii) The WF2 state is the stable state at zero field and at small opposite fields. When the field applied in the opposite direction is increased to a certain value, the reversal of magnetization occurs and the WF1 state is recovered, but with negative magnetization. This is the second step (WF2→WF1), for which the critical field corresponding to the coercive field. Summarizing, the stepped hysteresis loop may be described as a WF1→WF2→WF1→WF2→WF1 cycle of phase transitions upon cycling the field. It is noticeable that the original AF state is not involved in the cycle. The AF state can be recovered only by warming the magnetized sample to above T_C and then cooling it under zero field. The above model is reasonable based on the following considerations. The fact that the WF1→WF2 transition occurs at zero field for both compounds, independent of interlayer spacing, suggests that this transition dose not involve the breaking of the interlayer F ordering that is related to interlayer dipolar interactions. Otherwise, a field would be needed, the strength depending upon the interlayer spacing. It is likely that the WF1 state at low field assumes a multidomain structure, which is created by an anisotropy field exceeding the applied field. Then the WF1→WF2 step may corresponds to some reorientation of the microdomains upon decreasing the applied field to zero, and the interlayer F ordering is retained within the domains in the WF2 state. The WF2 state is stabilized by the internal anisotropy field related to interlayer dipolar interactions, and to induce the WF2→WF1 step (the reversal of magnetization), a sufficiently strong external field overcoming the internal field is needed. This justifies the coercivity of the materials. Clearly, the coercivity is strongly dependent upon the interlayer interaction and hence upon the interlayer separation, in good agreement with the greatly different coercive fields of **1** and **2**. The fact the magnetization for **2** at WF2 is much weaker than that for **1** at WF2 are also consistent with the model: larger interlayer spacing leads to weaker anisotropy field and hence stabilizes weaker magnetizations.

The hysteresis loops of **1** at 15 and 22 K suggest that the hysteresis coercive field decrease rapidly with temperature. The thermal effect is similar to that for the metamagnetic critical field. At 22 K, the absence of the metamagnetic transition and the hysteresis steps indicates the AF and WF2 states no longer exists, because the anisotropy fields that stabilize the states are vanishingly small at this temperature. To complete the remarks on hysteresis, we note that compound **3** does not exhibit stepped hysteresis, and the coercivity (120 Oe, polycrystalline sample at 2 K) is much weaker (the hysteresis behavior of **4** was not reported).[11b] The great differences of **3** from the present compounds, which are difficult to justify, illustrate the great impact of intralayer structures (combined with other factors). It must be noted that the hysteresis behaviors are influenced by particle shape and size,[13] Further studies, including magnetic characterization on single crystals and neutron diffraction on deuterated materials, are needed to confirm the above interpretation.

Finally, a few remarks on canting angles are worthwhile. According to the mechanisms of spin canting, the canting angle should mainly depend upon intralayer factors. However, from the data listed in Table 1, we cannot find any reliable correlation between the canting angles and the intralayer factors. Given the almost identical layer structures in **1** and **2**, we presume that the evident difference in canting angles (6.4° for **1** and 9.9° for **2**) is related to the anisotropic interlayer dipolar interactions, which may play an adjusting role. But it must be noted that these values of canting angles are rough estimations.

 © 2009 Wiley-VCH Verlag GmbH & Co. KGaA, Weinheim

Conclusions

We have described two multilayer molecular magnets in which azide-bridged Co^{II} layers are interlinked (**1**) by the btzb bidentate ligands or spaced (**2**) by the bilayered btze monodentate ligands. At high temperature (>25 K), almost identical magnetic behaviors typical of 2D AF systems are observed for **1** and **2**. Whereas at lower temperature, they exhibit unusual LRO behaviors combining spin canting (weak ferromagnetism), metamagnetism and stepped hysteresis. The structural feature contained within these two multilayer Co^{II} molecular magnets is that the two compounds have almost identical layer structures but with distinct interlayer separations (10.6 vs. 15.2 Å). This has allowed us to investigate in what aspects the interlayer separation influences the magnetic behaviors. It turns out that the interlayer separation has little influence on the ordering temperature (23 vs. 22 K), but imposes very strong influence on the metamagnetic critical field (6500 vs. 500 Oe), the coercivity (7500 vs. 650 Oe), and the hysteresis-step size. It is the first time that the influences of interlayer separations in the strongly anisotropic Co^{II}-azide systems are unambiguously determined.

The similarity and differences observed in **1** and **2** have also helped us to gain a better understanding of the complex magnetic behaviors. In particular, taking into account the strong anisotropy and the interlayer dipolar interactions, we have proposed that at least three states exist below T_C. i) An AF state with hidden spin-canting is obtained at low temperature by cooling under zero field. ii) The AF state can undergo the field-induced metamagnetic transition to generate a WF1 state, which exist under relatively high fields. iii) Upon switching off the applied field, the WF1 state relaxes to a different weak ferromagnetic state (WF2). The WF2 state possesses coercivity and undergoes magnetization reversal under the coercive field to recover the WF1 state. The unusual metamagnetic and hysteresis behaviors and the differences between **1** and **2** can be well interpreted by these considerations.

The findings in this work provide important information for the design of molecular magnetic materials, and demonstrate the potentials of controlling bulk magnetic properties (for example, coercivity) at the supramolecular level. Studies along this line may also help to further unveil the magnetic complexity and diversity in molecular systems.

Experimental Section

Materials and measurements: All reagents purchased were of reagent grade and used without further purification. The ligands btze and btzb were prepared according to literature methods.[21] FT-IR spectra were recorded in the range 500–4000 cm^{-1} on a Nicolet NEXUS 670 spectrophotometer using KBr pellets. Powder X-ray diffraction data were collected on a Bruker D8-ADVANCE diffractometer equipped with $Cu_{K\alpha}$ at a scan speed of $1°\,min^{-1}$.

Synthesis of $[Co(N_3)_2(btzb)]$ (1): A solution of NaN_3 (0.013 g, 0.20 mmol) in water (2 mL) was added into a mixture of $CoCl_2{\cdot}6H_2O$ (0.024 g, 0.10 mmol) and btzb (0.019 g, 0.10 mmol) in water (5 mL). After stirring for 5 min, the resulting clear solution was allowed to stand at room temperature, and red crystals of **1** were obtained in a week (52%). Elemental analysis calcd. (%) for $C_6H_{10}CoN_{14}$: C 21.4, H 3.0, N 58.2; found: C 21.5, H 3.3, N 58.4; IR (KBr): $\tilde{\nu}$=3131 (m), 2074 (vs), 1498 (m), 1443 (m), 1170 (m), 1097 (m), 1001 cm^{-1} (m).

Synthesis of $[Co(N_3)_2(btze)_2]$ (2): Crystals of **2** were obtained by a similar procedure, using btzb (0.032 g, 0.20 mmol) instead of btzb (65%). Elemental analysis calcd. (%) for $C_8H_{12}CoN_{22}$: C 20.2, H 2.6, N 64.8; found: C 21.3, H 2.9, N 64.8; IR (KBr): $\tilde{\nu}$=3132 (m), 2073 (vs), 1504 (m), 1452 (m), 1184 (m), 1097 (m), 1003 cm^{-1} (m).

Crystallographic determination: Diffraction intensity data were collected on a Bruker Apex II CCD area detector equipped with graphite-monochromated $Mo_{K\alpha}$ radiation (λ=0.71073 Å) at 293 K. Absorption corrections were applied using the multiscan program SADABS.[22] The structures were solved by the direct method and refined by the full-matrix least-squares method on F^2 using the SHELXTL program,[23] with anisotropic thermal parameters for all non-hydrogen atoms. The hydrogen atoms were placed in calculated positions and refined using the riding model. A summary of the crystallographic data is given in Table 2.

Table 2. Crystal data and structure refinements for complexes **1** and **2**.

Compound	**1**	**2**
formula	$C_6H_{10}CoN_{14}$	$C_8H_{12}CoN_{22}$
M_r	337.21	475.33
crystal system	monoclinic	monoclinic
space group	$P2_1/c$	$P2_1/c$
a [Å]	10.633(4)	15.172(4)
b [Å]	6.240(2)	6.2441(15)
c [Å]	9.764(3)	9.875(2)
β [°]	96.341(5)	101.175(3)
V [Å^3]	643.8(4)	917.8(4)
Z	2	2
ρ_{calcd} [g cm^{-3}]	1.740	1.720
μ [mm^{-1}]	1.354	0.989
unique reflections	1407	1975
R_{int}	0.0321	0.0237
R_1 [$I>2\sigma(I)$]	0.0331	0.0277
wR_2(all data)	0.0833	0.0651

CCDC 687570 (**1**) and 698720 (**2**) contains the supplementary crystallographic data for this paper. These data can be obtained free of charge from The Cambridge Crystallographic Data Centre via www.ccdc.cam.ac.uk/data_request/cif

Acknowledgements

The authors thank NSFC (20571026, 20771038 and 20490210), MOE (NCET-05-0425), Shanghai Leading Academic Discipline Project (B409), and STCSM (06SR07101) for financial support.

[1] a) D. Gatteschi, O. Kahn, J. S. Miller, F. Palacio, *Magnetic Molecular Materials*, Kluwer Academic, Dordrecht, **1991**; b) O. Kahn, *Molecular Magnetism*, VCH, New York, **1993**; c) J. S. Miller, *Adv. Mater.* **2002**, *14*, 1105; d) *Magnetism: Molecules to Materials, Vol. I–V* (Eds.: J. S. Miller, M. Drillon), Wiley-VCH, Weinheim, **2002–2005**; e) Special issue on Magnetism - Molecular, Supramolecular Perspectives-*Coord. Chem. Rev.* **2005**, *249*.

[2] a) D. Gatteschi, R. Sessoli, *Angew. Chem.* **2003**, *115*, 278; *Angew. Chem. Int. Ed.* **2003**, *42*, 268; b) G. Aromí, E. K. Brechin, *Struct.*

 © 2009 Wiley-VCH Verlag GmbH & Co. KGaA, Weinheim

Bonding (Berlin) **2006**, *122*; 1; c) C. Coulon, H. Miyasaka, R. Clérac, *Struct. Bonding (Berlin)* **2006**, *122*, 163.

[3] a) S. M. Humphrey, P. T. Wood, *J. Am. Chem. Soc.* **2004**, *126*, 13236; W.-K. Chang, R.-K. Chiang, Y.-C. Jiang, S.-L. Wang, S.-F. Lee, K.-H. Lii, *Inorg. Chem.* **2004**, *43*, 2564; b) E. Colacio, J. M. Domínguez-Vera, M. Ghazi, R. Kivekäs, F. Lloret, J. M. Moreno, H. Stoeckli-Evans, *Chem. Commun.* **1999**, 987.

[4] a) O. Sato, J. Tao, Y.-Z. Zhang, *Angew. Chem.* **2007**, *119*, 2200; *Angew. Chem. Int. Ed.* **2007**, *46*, 2152; b) E. Coronado, P. Day, *Chem. Rev.* **2004**, *104*, 5419; c) D. R. Talham, *Chem. Rev.* **2004**, *104*, 5479; d) D. Maspoch, D. Ruiz-Molina, K. Wurst, N. Domingo, M. Cavallini, F. Biscarini, J. Tejada, C. Rovira, J. Veciana, *Nat. Mater.* **2003**, *2*, 190; e) E.-Q. Gao, S.-Q. Bai, Z.-M. Wang, C.-H. Yan, *J. Am. Chem. Soc.* **2003**, *125*, 4984.

[5] a) J. Ribas, A. Escuer, M. Monfort, R. Vicente, R. Cortés, L. Lezama, T. Rojo, *Coord. Chem. Rev.* **1999**, *193–195*, 1027; b) X.-Y. Wang, Z.-M. Wang, S. Gao, *Chem. Commun.* **2008**, 281; c) E.-Q. Gao, Y.-F. Yue, S.-Q. Bai, Z. He, C.-H. Yan, *J. Am. Chem. Soc.* **2004**, *126*, 1419; d) T.-F. Liu, D. Fu, S. Gao, Y.-Z. Zhang, H.-L. Sun, G. Su, Y.-J. Liu, *J. Am. Chem. Soc.* **2003**, *125*, 13976; e) Y.-F. Zeng, J.-P. Zhao, B.-W. Hu, X. Hu, F.-C. Liu, J. Ribas, J. Ribas-Ariño, X.-H. Bu, *Chem. Eur. J.* **2007**, *13*, 9924.

[6] a) A. Escuer, G. Aromí, *Eur. J. Inorg. Chem.* **2006**, 4721; b) T. C. Stamatatos, K. A. Abboud, W. Wernsdorfer, G. Christou, *Angew. Chem.* **2007**, *119*, 902; *Angew. Chem. Int. Ed.* **2007**, *46*, 884; c) Y.-Z. Zhang, W. Wernsdorfer, F. Pan, Z.-M. Wang, S. Gao, *Chem. Commun.* **2006**, 3302; d) C. I. Yang, W. Wernsdorfer, G. H. Lee, H. L. Tsai, *J. Am. Chem. Soc.* **2007**, *129*, 456.

[7] a) A. Escuer, R. Vicente, M. A. S. Goher, F. A. Mautner, *Inorg. Chem.* **1996**, *35*, 6386; b) M. A. S. Goher, J. Cano, Y. Journaux, M. A. M. Abu-Youssef, F. A. Mautner, A. Escuer, R. Vicente, *Chem. Eur. J.* **2000**, *6*, 778; c) F. A. Mautner, R. Cortés, L. Lezama, T. Rojo, *Angew. Chem.* **1996**, *108*, 96; *Angew. Chem. Int. Ed. Engl.* **1996**, *35*, 78; d) S. Han, J. L. Manson, J. Kim, J. S. Miller, *Inorg. Chem.* **2000**, *39*, 4182; e) A.-H. Fu, X.-Y. Huang, J. Li, T. Yuen, C.-L. Lin, *Chem. Eur. J.* **2002**, *8*, 2239.

[8] a) P.-P. Liu, A.-L. Cheng, N. Liu, W.-W. Sun, E.-Q. Gao, *Chem. Mater.* **2007**, *19*, 2724; b) E.-Q. Gao, A.-L. Cheng, Y.-X. Xu, M.-Y. He, C.-H. Yan, *Inorg. Chem.* **2005**, *44*, 8822; c) E.-Q. Gao, Z.-M. Wang, C.-H. Yan, *Chem. Commun.* **2003**, 1748; d) X.-Y. Wang, L. Wang, Z.-M. Wang, S. Gao, *J. Am. Chem. Soc.* **2006**, *128*, 674.

[9] a) A. Escuer, R. Vicente, M. A. S. Goher, F. A. Mautner, M. A. M. Abu-Youssef, *Chem. Commun.* **2002**, 64; b) B.-Q. Ma, H.-L. Sun, S. Gao, G. Su, *Chem. Mater.* **2001**, *13*, 1946.

[10] a) E.-Q. Gao, Y.-F. Yue, S.-Q. Bai, Z. He, S.-W. Zhang, C. H. Yan, *Chem. Mater.* **2004**, *16*, 1590; b) A. Escuer, J. Cano, M. A. S. Goher, Y. Journaux, F. Lloret, F. A. Mautner, R. Vicente, *Inorg. Chem.* **2000**, *39*, 4688; c) X.-Y. Wang, L. Wang, Z.-M. Wang, G. Su, S. Gao, *Chem. Mater.* **2005**, *17*, 6369; d) A. Escuer, F. A. Mautner, M. A. S. Goher, M. A. M. Abu-Youssef, R. Vicente, *Chem. Commun.* **2005**, 605; e) M. A. S. Goher, M. A. M. Abu-Youssef, F. A. Mautner, J. R. Vicente, A. Escuer, *Eur. J. Inorg. Chem.* **2000**, 1819; f) B. Bitschnau, A. Egger, A. Escuer, F. A. Mautner, B. Sodin, R. Vicente, *Inorg. Chem.* **2006**, *45*, 868; g) M. A. M. Abu-Youssef, V. Langer, D. Luneau, E. Shams, M. A. S. Goher, L. Öhrström, *Eur. J. Inorg. Chem.* **2008**, 112; h) X.-T. Wang, Z.-M. Wang, S. Gao, *Inorg. Chem.* **2007**, *46*, 10452.

[11] a) M. A. M. Abu-Youssef, F. A. Mautner, R. Vicente, *Inorg. Chem.* **2007**, *46*, 4654; b) X.-Y. Wang, Z.-M. Wang, S. Gao, *Inorg. Chem.* **2008**, *47*, 5720.

[12] R. L. Carlin, *Magnetochemistry*, Springer-Verlag, Heidelberg, **1986**.

[13] a) M. G. F. Vaz, L. M. M. Pinheiro, H. O. Stumpf, A. F. C. Alcântara, S. Golhen, L. Ouahab, O. Cador, C Mathonière, O. Kahn, *Chem. Eur. J.* **1999**, *5*, 1486; b) M. Kurmoo, C. J. Kepert, *New J. Chem.* **1998**, *22*, 1515; c) C. Mathonière, C. J. Nuttall, S. Carling; P. Day, *Inorg. Chem.* **1996**, *35*, 1201.

[14] a) Z.-L. Huang, M. Drillon, N. Masciocchi, A. Sironi, J.-T. Zao, P. Rabu, P. Panissod, *Chem. Mater.* **2000**, *12*, 2805; b) V. Hardy, M. R. Lees, O. A. Petrenko, D. M. Paul, D. Flahaut, S. Hébert, A. Maignan, *Phys. Rev. B* **2004**, *70*, 064424; <lit c>R. Feyerherm, A. Loose, P. Rabu, M. Drillon, *Solid State Sci.* **2003**, *5*, 321.

[15] a) L. Carlucci, G. Ciani, D. M. Proserpio, *Coord. Chem. Rev.* **2003**, *246*, 247; b) X.-L. Wang, C. Qin, E.-B. Wang, Z.-M. Su, L. Xu, S. R. Batten, *Chem. Commun.* **2005**, 4789; c) X.-L. Wang, C. Qin, E.-B. Wang, Z.-M. Su, *Chem. Eur. J.* **2006**, *12*, 2680.

[16] a) P. Yin, S. Gao, L.-M. Zheng, Z.-M. Wang, X.-Q. Xin, *Chem. Commun.* **2003**, 1076; b) H. Jankovics, M. Daskalakis, C. P. Raptopoulou, A. Terzis, V. Tangoulis, J. Giapintzakis, T. Kiss, A. Salifoglou, *Inorg. Chem.* **2002**, *41*, 3366; c) A. Rujiwatra, C. J. Kepert, J. B. Claridge, M. J. Rosseinsky, H. Kumagai, M. Kurmoo, *J. Am. Chem. Soc.* **2001**, *123*, 10584.

[17] a) R. Feyerherm, A. Loose, T. Ishida, T. Nogami, J. Kreitlow, D. Baabe, F. J. Litterst, S. Süllow, H. H. Klauss, K. Doll, *Phys. Rev. B* **2004**, *69*, 134427; b) K. Nakayama, T. Ishida, R. Takayama, D. Hashizume, M. Yasui, F. Iwasaki, T. Nogami, *Chem. Lett.* **1998**, 497; c) S. Mossin, H. Weihe, H. O. Sørensen, N. Lima, R. Sessoli, *Dalton Trans.* **2004**, 632; d) K. Bernot, J. Luzon, R. Sessoli, A. Vindigni, J. Thion, S. Richeter, D. Leclercq, J. Larionova, A. van der Lee, *J. Am. Chem. Soc.* **2008**, *130*, 1619.

[18] a) I. Dzyaloshinsky, *J. Phys. Chem. Solids* **1958**, *4*, 241; b) T. Moriya, *Phys. Rev.* **1960**, *120*, 91; c) T. Moriya, *Phys. Rev.* **1960**, *117*, 635.

[19] a) P. Panissod, M. Drillon in *Magnetism—From Molecules to Materials, Volume IV* (Eds.: J. S. Miller, M. Drillon), Wiley-VCH, Weinheim, **2002**, pp. 233–269; b) M. Drillon, P. Panissod, *J. Magn. Magn. Mater.* **1998**, *188*, 93.

[20] a) M. Kurmoo, H. Kumagai, M. A. Green, B. W. Lovett, S. J. Blundell, A. Ardavan, J. Singleton, *J. Solid State Chem.* **2001**, *159*, 343; b) M. Kurmoo, H. Kumagai, S. M. Hughes, C. J. Kepert, *Inorg. Chem.* **2003**, *42*, 6709.

[21] a) P. J. van Koningsbruggen, Y Garcia, O. Kahn, L. Fournès, H. Kooijman, A. L. Spek, J. G. Haasnoot, J. Moscovici, K. Provost, A Michalowicz, F. Renz, P. Gütlich, *Inorg. Chem.* **2000**, *39*, 1891; b) P. J. van Koningsbruggen, Y Garcia, H. Kooijman, A. L. Spek, J. G. Haasnoot, O. Kahn, J. Linares, E. Codjovi, F. Varret, *J. Chem. Soc. Dalton Trans.* **2001**, 466.

[22] G. M. Sheldrick, Program for Empirical Absorption Correction of Area Detector Data; University of Göttingen, Germany, **1996**.

[23] G. M. Sheldrick, SHELXTL Version 5.1. Bruker Analytical X-ray Instruments, Madison, Wisconsin, USA, **1998**.

Received: August 21, 2008
Published online: December 19, 2008

 © 2009 Wiley-VCH Verlag GmbH & Co. KGaA, Weinheim